

Raman versus Non-Raman Behavior in Resonant Auger Spectra of HCl

E. Kukk, H. Aksela, and S. Aksela

Department of Physical Sciences, University of Oulu, FIN-90570 Oulu, Finland

F. Gel'mukhanov and H. Ågren

Institute of Physics and Measurement Technology, Linköping University, S-58183 Linköping, Sweden

S. Svensson

Department of Physics, Uppsala University, Box 530, S-75121 Uppsala, Sweden

(Received 13 July 1995)

Two different types of Auger processes are shown to constitute the resonant Auger spectra of HCl: one which does and one which does not show Raman narrowing with the decrease of the spectral width of the exciting radiation. An analytical explanation for this phenomenon is given. [S0031-9007(96)00044-0]

PACS numbers: 33.20.Fb, 33.20.-t

The Cl $2p$ absorption spectrum of the HCl molecule exhibits an intense well-defined pre-edge structure [1–3]. It consists of a broad feature around $h\nu = 200\text{--}203$ eV, known to be due to the excitations to the first unoccupied molecular orbital σ^* . This structure is accompanied by a series of sharp peaks at higher photon energies, corresponding to the excitations to s and d Rydberg orbitals. The relaxation of the core excitations can, in general, take place (i) through the resonant Auger decay in the molecular environment and (ii) through fast dissociation of the molecule, followed by atomic Auger decay. The character of the core-excited state determines the relaxation path and is therefore reflected in the structure and line shapes of the Auger electron spectrum.

The sharp absorption peaks correspond to the core-to-Rydberg excitations populating only a single energy state. The distribution of the exciting photons with energy ω is described by spectral function $\Phi(\omega - \omega_c, \gamma)$, which is centered at energy ω_c and has the width γ . If γ is so large that $\Phi(\omega - \omega_c, \gamma)$ can be taken as constant over the lifetime width Γ of the excited state, then the Auger electron lines reflect the lifetime broadening of the excited state [4]. The progress in the experimental techniques utilizing synchrotron radiation has made it possible to observe the Auger resonance Raman effect (ARRE) [5,6] in the vacuum ultraviolet range for free atoms [7] and recently also for molecules [8].

Resonant Auger constitutes a nonradiative x-ray scattering process in which the incoming x-ray photon with energy ω excites through dipole interaction D the molecule which then decays nonradiatively with emission of the Auger electron e^- due to Coulomb interaction Q . The amplitude of this process is given by the generalized Kramers-Heisenberg formula [6]:

$$F_{of}(\omega) \propto \sum_i \frac{\langle 0 | D | i \rangle \langle i | Q | f \rangle}{\omega - (E_i - E_0) + i(\Gamma/2)}, \quad (1)$$

where Γ is the lifetime width of the core excited state. We use here atomic units. The cross section of this process reads

$$\sigma(\epsilon, \omega) = \sum_f |F_{of}(\omega)|^2 \delta(\omega - \epsilon - (E_f - E_0)), \quad (2)$$

where E_0 and E_i are total molecular energies of ground and intermediate states, E_f is the total energy of the final state molecular ion, and ϵ is the energy of the Auger electron. A negligible lifetime width of the final state in the Auger process is then assumed. To describe a realistic experimental situation we must use the convolution $\bar{\sigma}(\epsilon, \omega_c)$ of the cross section (2) with the incoming x-ray photon spectral function $\Phi(\omega - \omega_c, \gamma)$. The presence of the Dirac δ -energy function in Eq. (2) implies that the ARRE becomes observable if γ is comparable with Γ . Under such experimental conditions, the Auger line shape is properly given by the product of the Lorentzian distribution of the lifetime broadening and the spectral function, which leads to the distorted shape and narrowing of the resonant Auger electron lines [4,9,10]. Obviously, if γ is much narrower than Γ , then the width of the Auger electron lines is practically determined by γ and linear dispersion of the Auger electron energy ϵ with ω_c can be observed.

The broadness of the molecular resonance features can be, in principle, a result of the repulsive nature of the excited state [11], or it can be due to the excitations to a manifold of close-lying vibronic levels of a bonding state. If the Auger decay of this manifold of states populates a single final state, then, just due to energy conservation, the Auger linewidth and energy ϵ must follow the spectral width γ and energy ω_c , even when $\gamma > \Gamma$.

The line-shape narrowing and linear dispersion, characteristic to the ARRE, have been observed by Liu *et al.* [8] for the Auger decay of the $3d^{-1}5p\pi$ Rydberg states in the HBr molecule. On the other hand, the Auger decay

of the $3d^{-1}\sigma^*$ state in the same molecule did not reveal any dispersive behavior of the line energies, excluding the possibility of the bonding nature of the $3d^{-1}\sigma^*$ excited state [12].

The different nature of the core-to- σ^* and core-to-Rydberg excitations in HCl can be seen as a striking difference between the electron spectra of the Auger decay of the $2p^{-1}\sigma^*$ and $2p^{-1}4s\sigma$ states [3]. The latter spectrum displays the term structure and vibronic properties characteristic of the molecular $2p^{-1}4s\sigma \rightarrow (4\sigma 5\sigma 2\pi)^{-2}4s\sigma$ resonant Auger transitions. In contrast, the former spectrum shows dominating atomiclike features, assigned to the $2p^{-1}3p^6 \rightarrow 3p^4$ Auger decay in the core-excited chlorine atom. It has been concluded that the $2p^{-1}\sigma^*$ states of the HCl molecule dissociate into neutral hydrogen and chlorine fragments, followed by the Auger decay. This conclusion is supported by ion yield measurements [13] and analogous findings for other hydrogen halides [12,14,15]. The repulsive character of the $2p^{-1}\sigma^*$ states has thus been shown by means of resonant Auger spectroscopy, in contrast to the bonding character of the $2p^{-1}4s\sigma$ and other Rydberg states. This result is in agreement with theoretical calculations of the potential energy curves for the excited states involved.

In this Letter, we present a comparative study of the high-resolution resonant Auger spectra taken at the $2p^{-1}\sigma^*$ and $2p^{-1}4s\sigma$ resonances of HCl and concentrate on the line narrowing and line-shape distortions, which are typical of the ARRE.

The spectra have been measured at the Finnish beam line at the MAX-Laboratory in Lund, Sweden [16]. Synchrotron radiation from a short-period undulator is monochromatized by a modified SX-700 monochromator [17]. The photon energy resolution has been varied using different exit slit widths. The spectra have been recorded with a hemispherical electron energy analyzer [18], operating at constant pass energy (20 eV) mode, which provides a 60–70 meV electron energy resolution.

Our present spectra support entirely the earlier conclusions about the fast dissociation of the $2p^{-1}\sigma^*$ states followed by the atomiclike Auger decay and about the molecular Auger decay of the $2p^{-1}4s\sigma$ states. Here, Fig. 1 presents only the most intense single Auger electron lines from the $2p_{3/2}$ excitations. The spectrum in panel (a) of Fig. 1 is taken at $\omega_c = 201.0$ eV, which corresponds to the $2p_{3/2} \rightarrow \sigma^*$ excitations. The selected Auger line results from the atomic $2p_{3/2}^{-1} \rightarrow 3p^{-2}(^1D)$ transition, following the fast $\text{HCl}(2p^5\sigma^*) \rightarrow \text{H}(1s) + \text{Cl}(2p^5 3p^6)$ dissociation. Panel (b) of Fig. 1 presents the $2p_{3/2}^{-1}4s\sigma \rightarrow 2\pi^{-2}(^1\Delta)4s\sigma$ Auger line taken at $\omega_c = 204.4$ eV, which is the energy of the $2p_{3/2} \rightarrow 4s\sigma$ Rydberg excitations. In addition, panel (c) shows the 2π photoelectron line, excited at $\omega_c = 204.4$ eV. The figure shows two sets of peaks from the spectra excited using 50 μm (\bullet) and 200 μm (\circ) monochromator exit slit widths, providing $\gamma = 100$ and 440 meV, respectively.

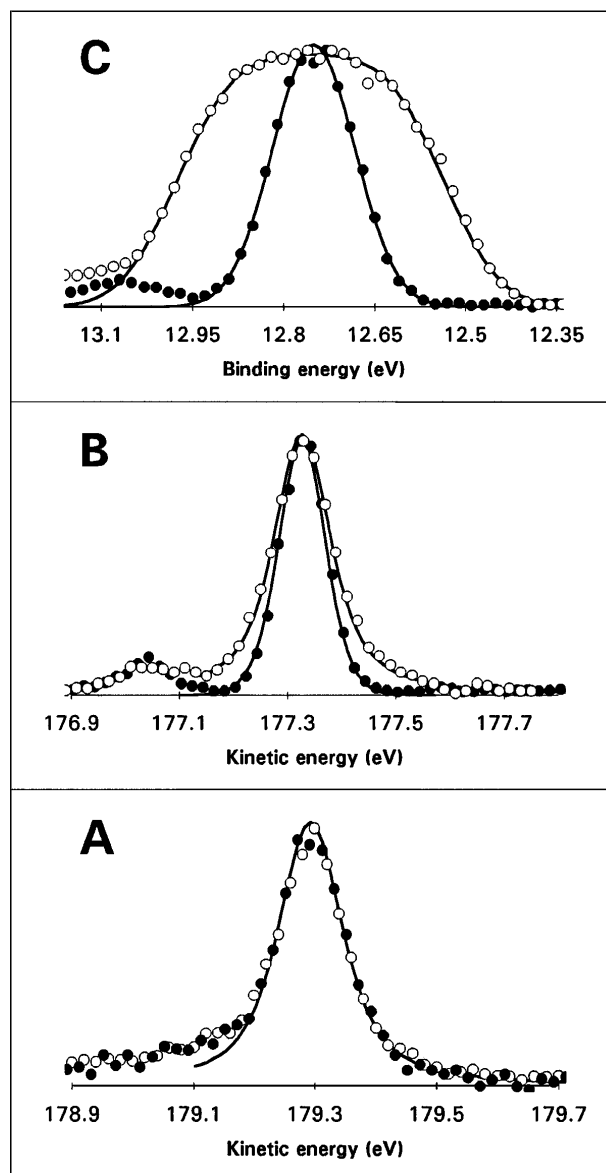


FIG. 1. Auger electron lines taken (a) at $2p \rightarrow \sigma^*$ resonance ($\omega_c = 201.0$ eV) and (b) at $2p \rightarrow 4s\sigma$ resonance ($\omega_c = 204.4$ eV). (c) The 2π photoelectron line taken at $\omega_c = 204.4$ eV.

As the lifetime width of the $2\pi^{-1}$ state is negligible, the 2π photoelectron line (c) follows the changes of γ and provides a good measure for the spectral function. The $3p^{-2}(^1D)$ Auger electron line (a) is completely insensitive to different spectral widths, whereas its analog in panel (b) of Fig. 1, the $2\pi^{-2}(^1\Delta)4s\sigma$ line, is strongly affected. Both Auger peaks in panel (a) have been fitted by an analytical function, obtained by convoluting the Lorentzian lifetime broadening with the Gaussian instrumental broadening (FWHM, 65 meV). The FWHM of 90 meV for the Lorentzian function has been used, as it leads to consistent fits for all the Auger peaks in Fig. 1

and is in good agreement with previous estimates for the core-hole lifetime [19,20]. The same analytical function gives a good fit also for the Auger peak (\circ) in panel (b), excited using a 200 μm exit slit. In this case γ is too large for the ARRE to be seen and the Auger line shape reflects the Lorentzian lifetime broadening of the core-excited state. The same Auger line is clearly narrower (with FWHM of about 100 meV) in the spectrum excited using 50 μm slit width (\bullet) and has a different line shape. In this case γ and Γ are comparable and the conditions to observe the ARRE have been reached. The fit curve for this peak is given by the product of the spectral function [curve (\bullet), panel (c), deconvoluted with the instrument function] and the lifetime Lorentzian broadening (FWHM, 90 meV), as described in Ref. [4]. The result is again convoluted with the instrument function to match the recorded spectrum. The excellent fit showing the typical cutoff of the Lorentzian "tails" clearly indicates the presence of the ARRE. Thus, it has been shown that the ARRE appears in the Auger decay of the $2p^{-1}4s\sigma$ state, but is missing in the decay of the $2p^{-1}\sigma^*$ state.

The presence of the ARRE in panel (b) of Fig. 1 can be explained by the fact that both of the two states participating in the decay process, the $2p^{-1}4s\sigma$ and the $2\pi^{-2}(1\Delta)4s\sigma$ states, have bound potentials [the $2\pi^{-2}(1\Delta)4s\sigma$ state is quasibound but with a very long lifetime [13]]. Because the final optical excited state has negligible lifetime the condition for ARRE as inferred by the δ -energy function in Eq. (2) is fulfilled, and the width of this Auger resonance is restricted only by the spectral width γ of the x-ray photons.

In the non-ARRE case, panel (a) of Fig. 1, the potential energy curve of the intermediate $2p^{-1}\sigma^*$ state is repulsive as we obtain from multiconfigurational self-consistent field calculations and as can be inferred from high-level calculations on the equivalent core ArH species [21] (the extremely shallow well predicted at 6 a.u. houses no bound vibrational levels and is of no consequence for the present analysis). A schematical plot of the potential energy curves of the intermediate and final states is given in Fig. 1. Because the final state is dissociative we need to consider the sum over final states (f) in Eq. (2) as a sum over final electronic states of the HCl^+ ion and an integral over momenta p (or energies $\epsilon_p = p^2/2\mu$) for the relative nuclear motion under dissociation. Here μ is the reduced molecular mass. The integration over final continuum nuclear states eliminates the δ function in the cross section (2) and leads to the following cross section for the continuum-continuum decay channel:

$$\sigma_{cc}(\epsilon, \omega) = \sum_f \sigma_f \exp\left[-\left(\frac{\omega - \epsilon - \Delta_f}{\gamma_c}\right)^2\right] \Delta(\epsilon - \epsilon_f, \Gamma), \quad (3)$$

where $\gamma_c = F_i a$, $a = 1/\sqrt{\mu\omega_0}$ is the average deviation of internuclear distance R from equilibrium distance R_0 , ω_0 is the ground state vibrational frequency, and $F_i = |(dU_i/dR)_0|$ is the slope of the interatomic potential

$U_i(R)$ of the intermediate electronic state at $R = R_0$ (it is assumed that the HCl molecule is excited from the zeroth vibrational level of the ground state). $\Delta_f = U_f(\infty) - U_0(R_0) + [U_i(R_0) - U_i(\infty)] - \omega_0/2$, where the potential energies of the ground state $U_0(R_0)$, intermediate state $U_i(R_0)$, $U_i(\infty)$, and final state $U_f(\infty)$ are defined as in Fig. 2. $\Delta(\epsilon - \epsilon_f, \Gamma)$ is the Lorentzian lifetime broadening of the intermediate resonance state, originating from the denominator in Eq. (1). σ_f is the contribution of the f th Auger resonance to the ARRE cross section.

The δ function in the general cross section (2) which causes the Raman resonance narrowing effect, is in Eq. (3) replaced by the Gaussian function at width γ_c describing the distribution of Franck-Condon factors (see Fig. 2). When γ_c is larger than the lifetime width Γ no resonance narrowing will be observed. Such a situation for monochromatic excitation with the photons of energy ω_c is illustrated in Fig. 2. The energy ϵ of the Auger electron can vary around ϵ_f , as the intermediate states with nuclear kinetic energy ϵ_p over the range of Γ get excited, each decaying to the final state with the same nuclear momentum.

The computed adiabatic $2p^{-1}\sigma^*$ potential of HCl gives an estimation of $\gamma_c \approx$ of 1.6 eV, thus well over the lifetime width $\Gamma \approx$ 90 meV (see Fig. 2). Also, the convolution of the cross section $\sigma_{cc}(\epsilon, \omega)$ with the spectral function, required to describe the experiment, has

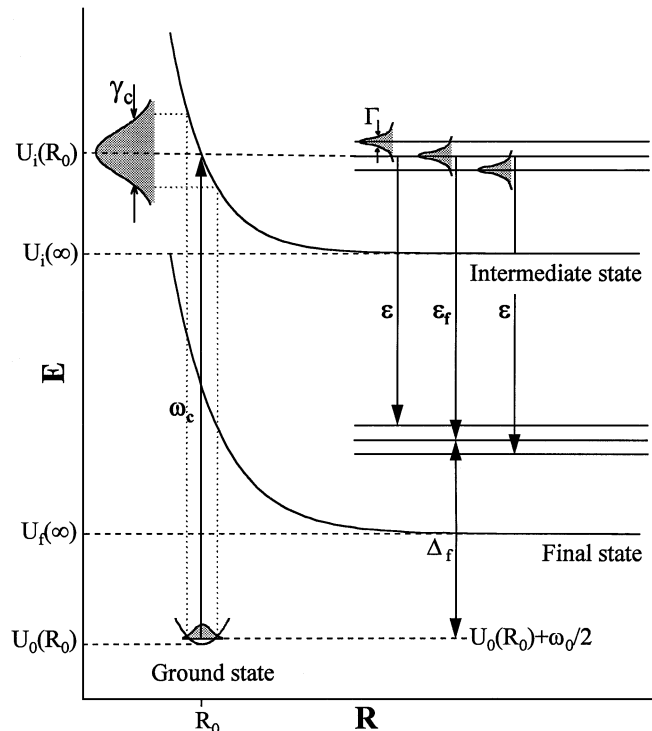


FIG. 2. A schematic diagram showing the potential energy curves and probability distributions, corresponding to the case of monochromatic excitation at the limit $\Gamma \ll \gamma_c$. For notations see text.

negligible effect, as $\Delta(\epsilon - \epsilon_f, \Gamma)$ does not depend on ω in Eq. (3) and the width γ_c of the Gaussian is much larger than the spectral width γ . The width of the Auger resonances for the considered case does therefore not depend on the width of spectral function γ but is limited only by the lifetime width Γ . In cases where γ_c is smaller than Γ , the resonance narrowing effect will take place.

Here we have considered the situation after the molecular dissociation has taken place. Because of the dissociation, a manifold of nuclear continuum states with different momenta p has become available for the intermediate resonance state, with a corresponding manifold in the Auger final state. From the viewpoint of the resonant Raman scattering, this availability of a wide spread of nuclear states leads to the vanishing of the resonant Raman narrowing in the Auger electron spectrum. An analogy can be drawn to the normal Auger decay following core ionization, where the excess energy is distributed between two electrons and thus the line narrowing is not observed. Here, a part of the available energy is carried away as the kinetic energy of the nuclear fragments.

We are grateful to Dr. Ergo Nömmiste, Dr. Olli-Pekka Sairanen, Dr. Andrus Ausmees, Stuart Osborne, and the staff of MAX-Laboratory for help in the measurements. Financial support from the Research Council for Natural Sciences of the Academy of Finland, the Swedish Natural Science Research Council (NFR), the Royal Swedish Academy of Sciences, and the University of Oulu is acknowledged.

-
- [1] W. Hayes and F. C. Brown, Phys. Rev. A **6**, 21 (1972).
 - [2] K. Ninomiya, E. Ishiguro, S. Iwata, A. Mikuni, and T. Sasaki, J. Phys. B **14**, 1777 (1981).
 - [3] A. Kivimäki, H. Aksela, S. Aksela, A. Yagishita, and E. Shigemasa, J. Phys. B **26**, 3379 (1993).

- [4] S. Aksela, E. Kukk, H. Aksela, and S. Svensson, Phys. Rev. Lett. **74**, 2917 (1995).
- [5] G. S. Brown, M. H. Chen, B. Crasemann, and G. E. Ice, Phys. Rev. Lett. **45**, 1937 (1980).
- [6] T. Åberg and B. Crasemann, in *X-Ray Resonant Anomalous Scattering* (Elsevier, Amsterdam, 1994).
- [7] A. Kivimäki, A. Naves de Brito, S. Aksela, H. Aksela, O.-P. Sairanen, A. Ausmees, S. J. Osborne, L. B. Dantas, and S. Svensson, Phys. Rev. Lett. **71**, 4307 (1993).
- [8] Z. F. Liu, G. M. Bancroft, K. H. Tan, and M. Schachter, Phys. Rev. Lett. **72**, 621 (1994).
- [9] F. Gel'mukhanov and H. Ågren, Phys. Lett. A **193**, 375 (1994).
- [10] G. B. Armen and H. Wang, Phys. Rev. A **51**, 1241 (1995).
- [11] S. Svensson, L. Karlsson, P. Balzer, B. Wannberg, U. Gelius, and M. Y. Adam, J. Chem. Phys. **89**, 7193 (1988).
- [12] P. Morin and I. Nenner, Phys. Rev. Lett. **56**, 1913 (1986).
- [13] H. Aksela, S. Aksela, M. Hotokka, A. Yagishita, and E. Shigemasa, J. Phys. B **25**, 3357 (1992).
- [14] P. Morin and I. Nenner, Phys. Scr. **T17**, 171 (1987).
- [15] Z. F. Liu, G. M. Bancroft, K. H. Tan, and M. Schachter, Phys. Rev. A **48**, R4019 (1993).
- [16] S. Aksela, A. Kivimäki, A. Naves de Brito, O.-P. Sairanen, S. Svensson, and J. Väyrynen, Rev. Sci. Instrum. **65**, 831 (1994).
- [17] S. Aksela, A. Kivimäki, R. Nyholm, and S. Svensson, Rev. Sci. Instrum. **63**, 1252 (1992).
- [18] S. J. Osborne, A. Ausmees, J. O. Forsell, B. Wannberg, G. Bray, L. B. Dantas, S. Svensson, A. Naves de Brito, A. Kivimäki, and S. Aksela, Synchrotron Radiat. News **7**, 25 (1994).
- [19] L. Karlsson, P. Baltzer, S. Svensson, and B. Wannberg, Phys. Rev. Lett. **60**, 2473 (1988).
- [20] H. Aksela, E. Kukk, S. Aksela, O.-P. Sairanen, A. Kivimäki, E. Nömmiste, A. Ausmees, S. J. Osborne, and S. Svensson, J. Phys. B **28**, 4259 (1995).
- [21] H. Partridge, D. W. Schwenke, and C. W. Bauschlicher, Jr., J. Chem. Phys. **99**, 9776 (1993).